© 2014. Published by The Company of Biologists Ltd | Development (2014) 141, 4127-4138 doi:10.1242/dev.107425

RESEARCH ARTICLE

A conserved role for non-neural ectoderm cells in early neural development

Marieke Cajal[1], Sophie E. Creuzet[2], Costis Papanayotou[1], Délara Sabéran-Djoneidi[1], Susana M. Chuva de Sousa Lopes[3], An Zwijsen[4], Jérôme Collignon[1] and Anne Camus[1,*]

ABSTRACT

During the early steps of head development, ectodermal patterning leads to the emergence of distinct non-neural and neural progenitor cells. The induction of the preplacodal ectoderm and the neural crest depends on well-studied signalling interactions between the non-neural ectoderm fated to become epidermis and the prospective neural plate. By contrast, the involvement of the non-neural ectoderm in the morphogenetic events leading to the development and patterning of the central nervous system has been studied less extensively. Here, we show that the removal of the rostral non-neural ectoderm abutting the prospective neural plate at late gastrulation stage leads, in mouse and chick embryos, to morphological defects in forebrain and craniofacial tissues. In particular, this ablation compromises the development of the telencephalon without affecting that of the diencephalon. Further investigations of ablated mouse embryos established that signalling centres crucial for forebrain regionalization, namely the axial mesendoderm and the anterior neural ridge, form normally. Moreover, changes in cell death or cell proliferation could not explain the specific loss of telencephalic tissue. Finally, we provide evidence that the removal of rostral tissues triggers misregulation of the BMP, WNT and FGF signalling pathways that may affect telencephalon development. This study opens new perspectives on the role of the neural/non-neural interface and reveals its functional relevance across higher vertebrates.

KEY WORDS: Embryo, Forebrain patterning, Signalling centre, Telencephalon, Apoptosis, Vertebrates, Mouse, Chick

INTRODUCTION

Experimental embryology and genetics have advanced our understanding of the early aspects of forebrain development (Andoniadou and Martinez-Barbera, 2013; Wilson and Houart, 2004). This complex structure is at the origin of the telencephalon, the optic vesicles, the hypothalamus and the diencephalon. The early steps of forebrain formation take place between pre-gastrula and late neural plate stages, and comprise a succession of interconnected events: the initial specification of an anterior character, the neural induction, and the early regionalization and patterning of the anterior neural plate (ANP). Progressive specification of anterior-posterior (A-P) and dorsoventral (D-V) neural patterning is achieved through the cooperation of signals from the anterior visceral endoderm (AVE) and from the organizer and its derivatives: the anterior definitive endoderm (ADE) and the axial mesendoderm (AME) (Arkell and Tam, 2012; Stern and Downs, 2012). The ADE and the AME promote neuralization and are sources of antagonistic activities that protect the anterior neural tissue from the caudalizing influence of WNTs, BMPs, Nodal and retinoic acid (Bachiller et al., 2000; del Barco Barrantes et al., 2003; Camus et al., 2000; Hallonet et al., 2002; Martinez Barbera et al., 2000; Shawlot et al., 1999). Once gastrulation is completed, additional mechanisms within the neural tissue itself become essential to counteract these caudalizing signals and prevent the posterior transformation of the ANP (Andoniadou et al., 2007; Arkell et al., 2013; Bayramov et al., 2011; Fossat et al., 2011; Houart et al., 2002; Lagutin et al., 2003; Paek et al., 2011).

The role of the non-neural ectoderm that abuts the rostralmost neural ectoderm in the early phase of ANP development is unclear. It is well known that neural crest cell (NCC) specification crucially depends on planar signals between the non-neural ectoderm and the prospective neural plate (Khudyakov and Bronner-Fraser, 2009; Patthey and Gunhaga, 2011; Selleck and Bronner-Fraser, 1995). NCCs are induced along the lateral borders of the neural plate but not rostrally (Carmona-Fontaine et al., 2007). Whether planar signals within this area could also be involved in the specification and regionalization of the ANP remains to be addressed (Papalopulu and Kintner, 1993).

Fate-mapping studies revealed the existence in different vertebrate species of a transitional zone at the rostral end of the neural plate at late gastrulation stages (Cajal et al., 2012; Ezin et al., 2009; Houart et al., 1998; Sanchez-Arrones et al., 2012; Streit, 2004). This zone is called ANB (anterior neural border) in zebrafish, APT (anterior proneural transitional ectoderm) in chick and INT (intermediate zone) in mouse. This border region contributes to both neural and non-neural derivatives, including the dorsal region of the forebrain and the neighbouring non-neural ectoderm at the origin of the adenohypophyseal and olfactory placodes, and other epidermal derivatives. The remodelling of this region and subsequent segregation of neural and non-neural subpopulations precedes the differentiation of the anterior neural ridge (ANR), a secondary organizer, at early somite stage. The ANR is essential for the regionalization of the forebrain and in particular for the formation of the telencephalon (Eagleson and Dempewolf, 2002; Kiecker and Lumsden, 2012; Vieira et al., 2010). *In vivo* ablation of ANB cells during gastrulation in zebrafish or of the ANR in ANP explants at early somite stage in mouse both lead to a failure of telencephalon induction (Houart et al., 1998; Shimamura and Rubenstein, 1997). In mouse embryos, the rostralmost non-neural ectoderm lying between the extra-embryonic ectoderm and the transitional zone is fated to become surface and buccal ectoderm (Cajal et al., 2012). Whether these non-neural ectoderm cells influence the development of the ANP and its subsequent regionalization is unknown. In this

[1]Université Paris Diderot, Sorbonne Paris Cité, Institut Jacques Monod, UMR7592 CNRS, Paris F-75013, France. [2]Institut de Neurobiologie, Laboratoire Neurobiologie et Développement, CNRS-UPR3294, avenue de la Terrasse, Gif-sur-Yvette 91198, France. [3]Department of Anatomy and Embryology, Leiden University Medical Centre, Leiden 2333 ZC, The Netherlands. [4]Laboratory of Developmental Signaling, VIB Center for the Biology of Disease, and KU Leuven, Department for Human Genetics, Leuven 3000, Belgium.

*Author for correspondence (camus.anne@ijm.univ-paris-diderot.fr)

Received 30 December 2013; Accepted 25 August 2014

Development (2014) 141, 4127-4138 doi:10.1242/dev.107425

study, we characterized the consequences of the *in vivo* ablation of the proximal anterior midline that comprises the rostralmost non-neural ectoderm cells to examine their implication in the early steps of ANP formation.

We found that the removal of the proximal anterior midline at late gastrulation in the mouse embryo leads to severe morphological defects in forebrain and presumptive craniofacial tissues. A detailed gene expression analysis showed that the anterior head truncation is mainly due to the absence of the telencephalon territory and is accompanied by impaired cephalic NCC (CNCC) migration. Importantly, AME and ANR developed normally in ablated embryos. Remarkably, a similar head phenotype was observed in the chick following the removal of the anterior non-neural ectoderm at comparable stages of development. These ablations triggered extensive apoptosis throughout the cephalic neuroectoderm. However, chemical prevention of apoptosis in ablated mouse embryos could not rescue telencephalic development. Hence, apoptosis does not explain the specific loss of telencephalon territory. By contrast, we show that the ablation results in defective BMP, WNT and FGF signalling that may compromise the emergence of the telencephalon. This study highlights an important requirement for the rostral non-neural ectoderm in the early regionalization of the forebrain territory before the establishment of the ANR signalling centre in mammalian and avian embryos.

RESULTS

Ablation of the proximal anterior midline results in severe head defects in the mouse embryo

To investigate the function of the rostral non-neural ectoderm in the development of the mouse ANP, we performed the ablation of the most proximal anterior midline tissues comprising the three germ layers (PROX embryo; Fig. 1A,B). According to the fate map of the anterior midline ectoderm (Cajal et al., 2012), the ablation removed the rostral non-neural ectoderm while leaving forebrain and ANR precursors intact. This ablation is different from the one performed in a previous study in which a rostral segment encompassing the prospective forebrain and rostral midbrain domains was removed (Camus et al., 2000). Control embryos were slit laterally through the three germ layers. Following manipulation, embryos were cultured *in vitro* and examined 6, 12 or 30 h later.

The effective removal of the targeted area was confirmed by whole-mount *in situ* hybridization on embryos fixed immediately after the ablation using the non-neural marker *Dlx5* (Fig. 1C), the expression of which correlates with prospective surface and buccal ectoderm cells (Cajal et al., 2012). Head development is maintained by the anterior AME, which comprises the ADE and the prechordal plate (Camus et al., 2000). In the present study, our ablation strategy leaves the prospective prechordal plate intact, as demonstrated by *Gsc* expression (Fig. 1D). Remarkably, after 6 h of culture, the non-neural ectoderm population was reconstituted *de novo* at the midline, as demonstrated by the expression of *Dlx5*, and was the same in PROX and control embryos after 12 h (Fig. 1E-H). Furthermore, the analysis of *Hesx1* expression showed that the already specified anterior neural progenitors were not depleted and remained unaffected in PROX embryos after 6 and 12 h of culture (Fig. 1I-L).

Morphological defects in PROX embryos were first seen when they reached the 1- to 3-somite stage (compare Fig. 1G,K to H,L). After 30 h of culture, 70% of the PROX embryos differed from control embryos by the presence of heart bifida and a truncated head region developing outside of the amnion and visceral yolk sac (VYS) membranes (Fig. 1M,N; supplementary material Fig. S1A). The forebrain appeared severely reduced and the optic vesicles were not visible. The midbrain and hindbrain also seemed reduced in size, although to a lesser extent. Additional control experiments were performed at this stage, involving either an anterior 'slit' at the extra-embryonic/embryonic boundary or the ablation of the anterior distal extra-embryonic midline region (supplementary material Fig. S1B-E). All these operated embryos developed normally without showing head truncation.

We questioned whether the head phenotype observed in PROX embryos resulted from a defect in the development of the AME. *Dkk1* and *Cerl* expressions were detected in PROX embryos at 6 and 12 h of culture, suggesting that the ADE developed normally (Fig. 1O-T). The prechordal plate was also formed at the anterior part of the AME, as shown by *Gsc* expression in PROX embryos at 6 and 12 h of culture (Fig. 1U-X). Finally, *Shh* expression along the entire AME was comparable between PROX and control embryos at 30 h of culture (Fig. 1Y,Z). These results indicate that the removal of the proximal anterior midline results in a truncation of the head without compromising AME formation.

Neuroectoderm, surface ectoderm and NCCs are specified, despite the removal of proximal anterior midline

The severe head truncation observed in PROX embryos was suggestive of neural and craniofacial defects. We performed whole-mount *in situ* hybridization and histology to assess the specification and morphogenesis of neuroectoderm, surface ectoderm, preplacodal tissue and NCCs in ablated embryos at the cephalic level. Despite the severe anterior truncation, these tissues were properly specified in PROX embryos (Fig. 2A-H). Histological analysis confirmed that *Sox1*, *Dlx5*, *Tfap2c* and *Sox10* genes are transcribed in distinct domains, even though tissue morphology is highly disturbed compared with control (Fig. 2A′-H′; supplementary material Fig. S2). Forebrain and midbrain neuroectoderm surface was reduced by 40% in PROX embryos compared with controls after 30 h in culture (n=19 PROX and n=9 control; supplementary material Fig. S2A,B; data not shown).

Sox10-positive emigrating CNCCs reached the first branchial arch (BA1) but were absent more rostrally, indicating that their survival or migration is affected in PROX embryos (Fig. 2G,H). Note that BA1, which normally becomes apparent between the 6- and 8-somite stages, was reduced in PROX embryos. CNCCs originate at a more caudal position than the ablated region in PROX embryos (Cajal et al., 2012). Therefore, we excluded the hypothesis that the primary defects observed in the ANP are due to an early depletion of CNCCs. Migratory and/or survival defects of the CNCCs in PROX embryos may be a consequence of the anterior head truncation and in turn may influence the morphogenesis and growth of the forebrain from the 5- to 6-somite stage onward as it has been indicated by experiments in the chick embryo (Creuzet, 2009).

The proximal anterior midline is dispensable for early AP patterning and the establishment of secondary organizers

Transcription factors SIX3 and IRX3 distinguish subregions of the ANP with distinct developmental fates (Braun et al., 2003; Kobayashi et al., 2002). Despite the fairly reduced *Six3*-positive territory present in PROX embryos compared with controls, adjacent and non-overlapping expression domains of *Six3* and *Irx3* were observed by whole-mount *in situ* hybridization after 30 h of culture (Fig. 3A-E). It has been shown that surgical removal of the ANR or treatment of forebrain explants with inhibitors of FGF signalling causes the loss of anterior areas in the forebrain

Development (2014) 141, 4127-4138 doi:10.1242/dev.107425

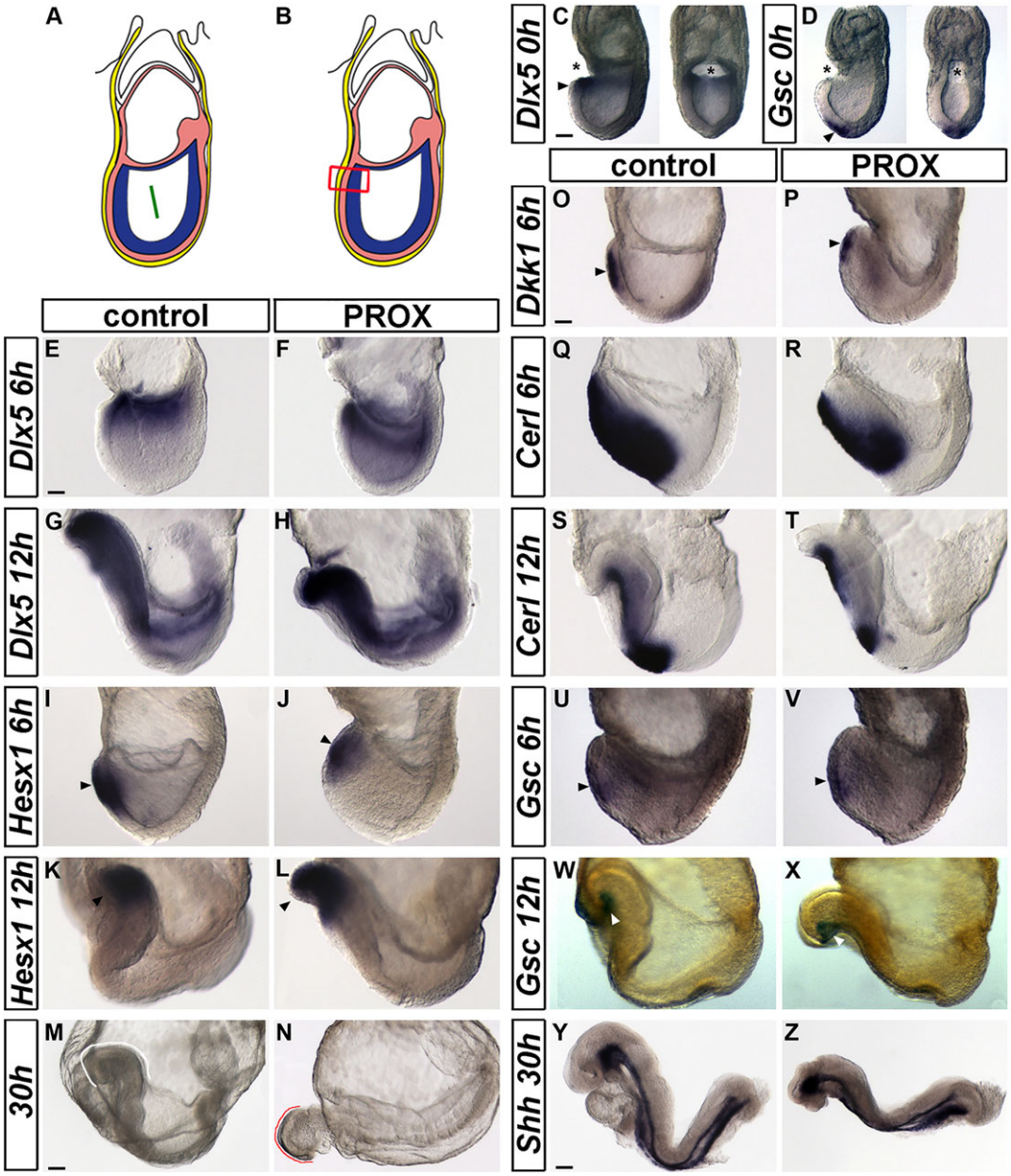

Fig. 1. Ablation of the proximal anterior midline in E7.5 mouse embryos. (A,B) Schematic representation of the micromanipulations in OB/EB stage embryos. (A) Control embryos with a lateral cut (green bar). (B) PROX embryos where the three germ layers of the most proximal anterior midline are ablated (red square). The ablation removes surface and buccal ectoderm progenitor cells, as well as prospective foregut and cardiac mesoderm cells. (C,D) *Dlx5* and *Gsc* expression (arrowheads) in PROX embryos fixed immediately after ablation (asterisks) in lateral (left) and frontal (right) views. (E-H) *Dlx5* expression in control (E,G) and PROX (F,H) embryos cultured for 6 and 12 h. The variation seen in *Dlx5* pattern between PROX and control embryos is due to slight differences in the embryonic stages. (I-L) *Hesx1* expression in control (I,K) and PROX (J,L) embryos cultured for 6 and 12 h. (M,N) Morphology of control (M) and PROX (N) embryos cultured for 30 h. The head of the PROX embryo (red contour line) is truncated compared with the control (white contour line) and displays an abnormal rounded shape and atypical ventral flexure at the hindbrain level. (O,P) *Dkk1* expression in control (O) and PROX (P) embryos cultured for 6 h. (Q-T) *Cerl* expression in control (Q,S) and PROX (R,T) embryos cultured for 6 and 12 h. (U,V) *Gsc* expression in control and PROX embryos cultured for 6 h. (W,X) Control and PROX *Gsc+/lacZ* embryos showing β-galactosidase activity in the prechordal plate cultured for 12 h. (Y,Z) *Shh* expression in control and PROX embryos cultured for 30 h. Scale bars: 80 µm in C,D; 50 µm in E-L,O-X; 90 µm in M,N; 70 µm in Y,Z.

(Shimamura and Rubenstein, 1997; Ye et al., 1998). Although our ablation does not remove ANR precursors (Cajal et al., 2012), it may affect their survival and final allocation within the ANP. We show that *Fgf8* expression was detected in the ANR and in the isthmic organizer (IsO) at the midbrain-hindbrain boundary in PROX embryos after 30 h of culture (Fig. 3F-G″). Remarkably, the expression of *Fgf8* was expanded rostrally in the majority of the PROX embryos (n=12/17), whereas it was unaltered at the level of the IsO. We conclude that the specification of secondary organizers and the initial A-P organization of the neural tube do take place in ablated embryos.

The proximal anterior midline is crucial for forebrain patterning and telencephalon specification

In order to characterize further the defects, we assessed changes in the expression 30 h after ablation of several key genes required

Development (2014) 141, 4127-4138 doi:10.1242/dev.107425

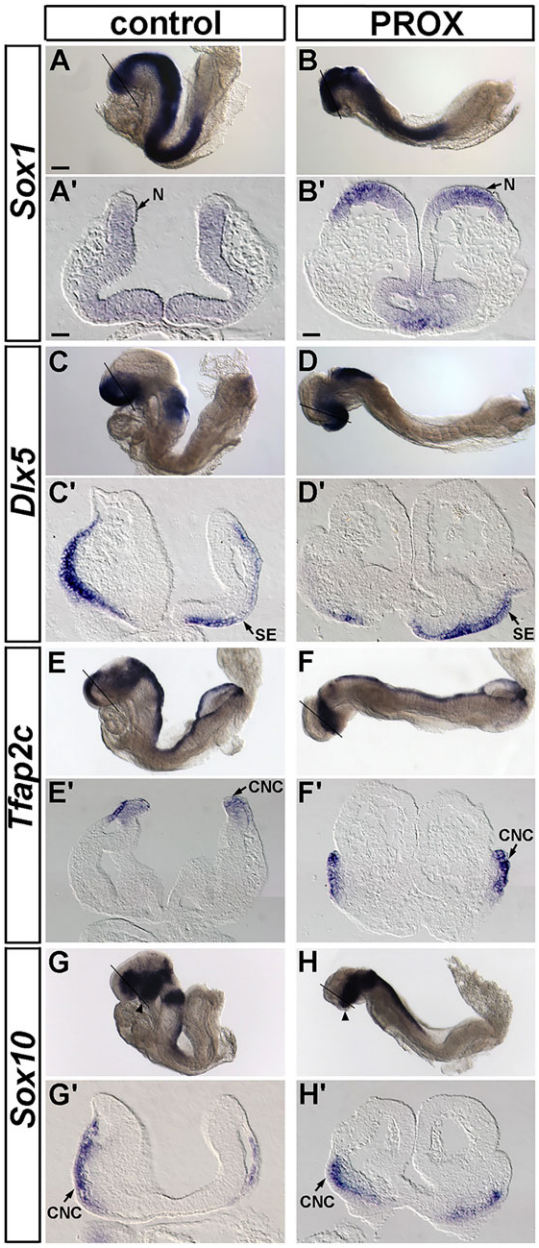

Fig. 2. Molecular analysis of neural and non-neural tissues of the forming head of ablated mouse embryos. (A-H) Whole-mount images and (A′-H′) frontal sections of control and PROX embryos cultured for 30 h showing *Sox1* (A-B′), *Dlx5* (C-D′), *Tfap2c* (E-F′) and *Sox10* (G-H′) expression. Section planes for A′-H′ are represented in A-H. In PROX embryos, *Sox10*-positive CNCCs do not migrate beyond the first branchial arch (black arrowhead). N, neuroectoderm; SE, surface ectoderm; CNC, cephalic neural crest. Scale bars: in A, 90 µm for A-H; in A′, 30 µm for A′,C′,G′,H′; in B′, 40 µm for B′,D′,E′,F′.

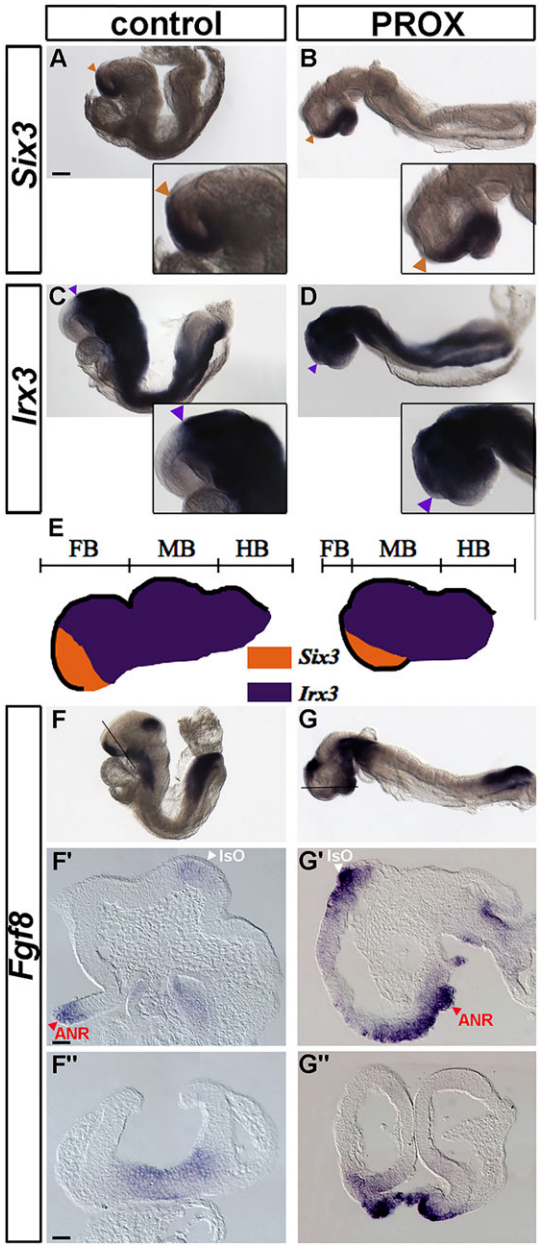

Fig. 3. Effect of removing the proximal anterior midline on molecular regionalization and secondary organizer establishment in mouse embryos. (A-D) Control (A,C) and PROX (B,D) embryos cultured for 30 h showing non-overlapping *Six3* (A,B) and *Irx3* (C,D) expression domains. Higher magnifications of the cephalic region are shown. Coloured arrowheads indicate *Six3* caudal (orange) and *Irx3* rostral (purple) expression boundaries. (E) Schematic representation of *Six3* and *Irx3* expression domains in control and PROX embryos. (F-G″) Expression of *Fgf8* in whole-mount (F,G) and on longitudinal (F′,G′) and frontal (F″,G″) sections. Section planes for F″,G″ are shown in F,G. ANR, anterior neural ridge; IsO, isthmic organizer. Scale bars: in A, 80 µm for A-D,F,G; 30 µm in F′; in F″, 25 µm for F″,G′,G″.

for anterior development. In agreement with morphological observations, the extent of the expression of the forebrain and midbrain marker *Otx2* appeared reduced (Fig. 4A,B). Furthermore, the analysis of *Hesx1* expression confirmed that the forebrain territory was reduced in PROX embryos (Fig. 4C,D). Finally, the *Wnt1* expression domain of prospective posterior diencephalon, midbrain and hindbrain appeared shifted anteriorly, and abutted the *Nkx2.1* expression domain in the ventral diencephalon (Fig. 4E-I). This indicates that the telencephalic territory is severely reduced in size in PROX embryos.

The loss of telencephalic tissue was confirmed by a decrease in the expression of specific regional markers such as *Emx2, Pax6* and *Wnt8b*. However, some expression of these genes persisted at a rostral and ventral position where the expression of *Vax1* and *Foxg1* was also detected (Fig. 5A-J). Histological analysis of PROX embryos showed that *Foxg1*-positive telencephalic expression was greatly diminished whereas *Foxg1* expression remained present in ANR and prospective olfactory placodes, and that this was also the case for the

Development (2014) 141, 4127-4138 doi:10.1242/dev.107425

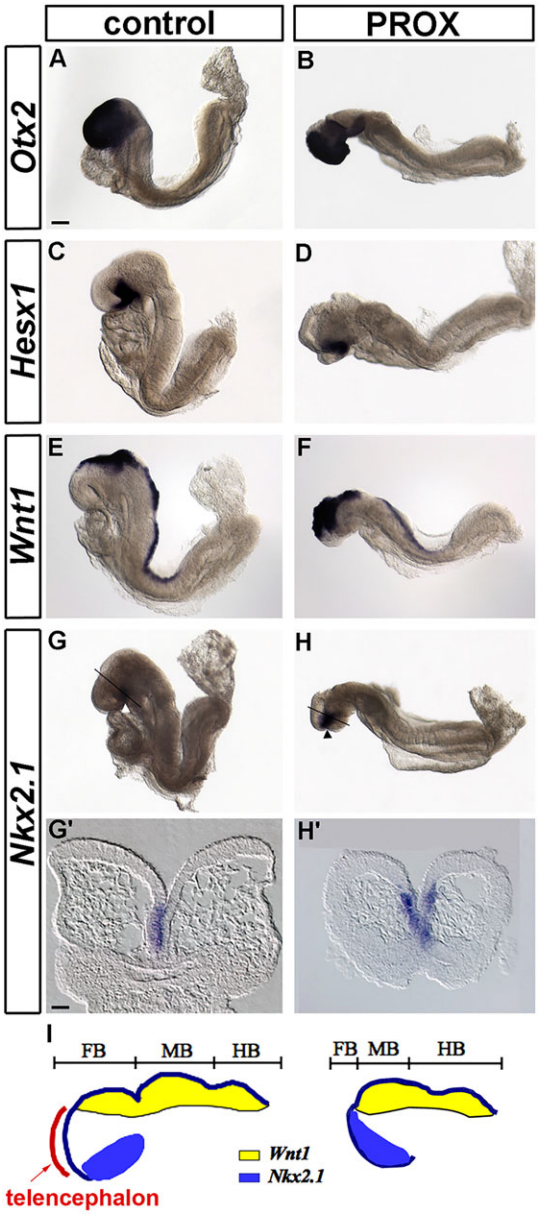

Fig. 4. Comparative gene expression analysis of the developing head in control and ablated mouse embryos. (A-H′) Whole-mount images (A-H) and frontal sections (G′,H′) of control and PROX embryos cultured for 30 h showing *Otx2*, *Hesx1*, *Wnt1* and *Nkx2.1* expression. The comparison of *Wnt1* (E,F) and *Nkx2.1* (G, arrowhead in H) expression domains in PROX and control embryos confirms the lack of telencephalon. Section planes for G′,H′ are indicated in G,H. (I) Schematic representation of *Wnt1* and *Nkx2.1* expression domains in control and PROX embryos. Scale bars: in A, 80 µm for A-H; in G′, 30 µm for G′,H′.

expression of *Vax1* (Fig. 5I′-J″; supplementary material Fig. S3). Taken together, these results indicate that the telencephalon territory is severely reduced or lost whereas diencephalic tissues are less altered (Fig. 4G′,H′). Finally, whole-mount *in situ* hybridization and histological analysis of the ventral diencephalon and optic vesicles marker *Rax* demonstrated that the eye field is specified but reduced (Fig. 5K-L″). These findings are summarized in a diagram highlighting the topographical changes caused by the ablation (Fig. 6A,B). The quantitative expression study of individual embryos was consistent with the observations made by whole-mount *in situ* hybridization (Fig. 6C). The comparison of the normalized values obtained for control and PROX embryos revealed a significant reduction in the expression of anterior and dorsal forebrain markers in PROX embryos. By contrast, ventral diencephalon and midbrain markers were not significantly diminished. Altogether, these results demonstrate that PROX embryos exhibit specific defects in the establishment of the forebrain and in particular of the telencephalon territory.

Ablation of anterior non-neural ectoderm cells results in neural and craniofacial defects in the chick embryo

In the E7.5 mouse embryo, the PROX ablation inevitably removes tissue from the three germ layers, as ectoderm cannot be mechanically separated from the mesoderm and the endoderm at the midline. By contrast, it is technically possible to excise the ectoderm layer without affecting other germ layers in the chick embryo at stage 4 (HH4), when the primitive streak is at its maximum elongation. Taking advantage of this refinement of the ablation, we characterized the phenotype of anterior non-neural ectoderm-ablated chick embryos (NNE embryos; Fig. 7A,B). The fate map of the chick cephalic neural fold served as a reference for the manipulation (Fernandez-Garre et al., 2002; Puelles et al., 2005; Sanchez-Arrones et al., 2009, 2012). NNE embryos developed within the amnion and VYS, and cardia bifida was never observed except when the subjacent endoderm layer was altered. NNE embryos harvested 32 h after the ablation had reached 22 somites (HH14) and displayed a microcephaly (n=35; Fig. 7C,D). In addition, severe reductions of the optic vesicles and the branchial arches were observed. The forebrain, together with the midbrain, remained as a simple neural tube, without undergoing the stereotypical dorsolateral growth leading to the formation of cephalic vesicles, as seen in controls (n=47; Fig. 7C,D).

The ablation did not affect the specification of neural ectoderm: Sox2 activity was similar in both control and ablated embryos shortly after operation (n=12 and n=18, respectively; Fig. 7E,F). In addition, the formation of head process was not perturbed, as attested by Not1 immunolabelling (n=18; Fig. 7E,F). When harvested later (50 h), the brain appeared dramatically everted in HH18 NNE embryos, as shown by Sox2 (n=15 and n=10 for control embryos; Fig. 7G,H). The abnormal development of the forebrain and in particular of the telencephalon territory was further demonstrated by the reduction of the *Foxg1* and *Six3* expression domains at HH18 (n=11 and n=12, respectively; Fig. 7I-N). Although in controls *Foxg1* transcripts were detected throughout the telencephalic neuroepithelium (n=9), their accumulation in ablated embryos was confined to the neural border. This condition was reminiscent of the situation encountered at neurula stage, where *Foxg1* expression is first detected in the ANR, before expanding in telencephalic anlage. Similarly, *Pax6* expression in prosencephalic vesicles was shifted to the neural border of everted brains (n=11; Fig. 7O,P). In addition, the expression *Emx2* and *Otx2*, markers for dorsal telencephalic and di-mesencephalic development respectively, was vestigial in operated embryos (n=14 and n=11, respectively; Fig. 7Q-T). We conclude that the anterior non-neural ectoderm is required in HH4 chick embryos for the molecular specification of the prosencephalon and in particular for the emergence of the telencephalon. Its removal resulted in morphological defects similar to those observed in mouse embryos following the removal of the three germ layers of the proximal anterior midline.

Cell death and proliferation alterations do not account for the loss of telencephalon

To determine whether the loss of forebrain tissues in ablated mouse embryos is caused by reduced growth, cellular proliferation was

Development (2014) 141, 4127-4138 doi:10.1242/dev.107425

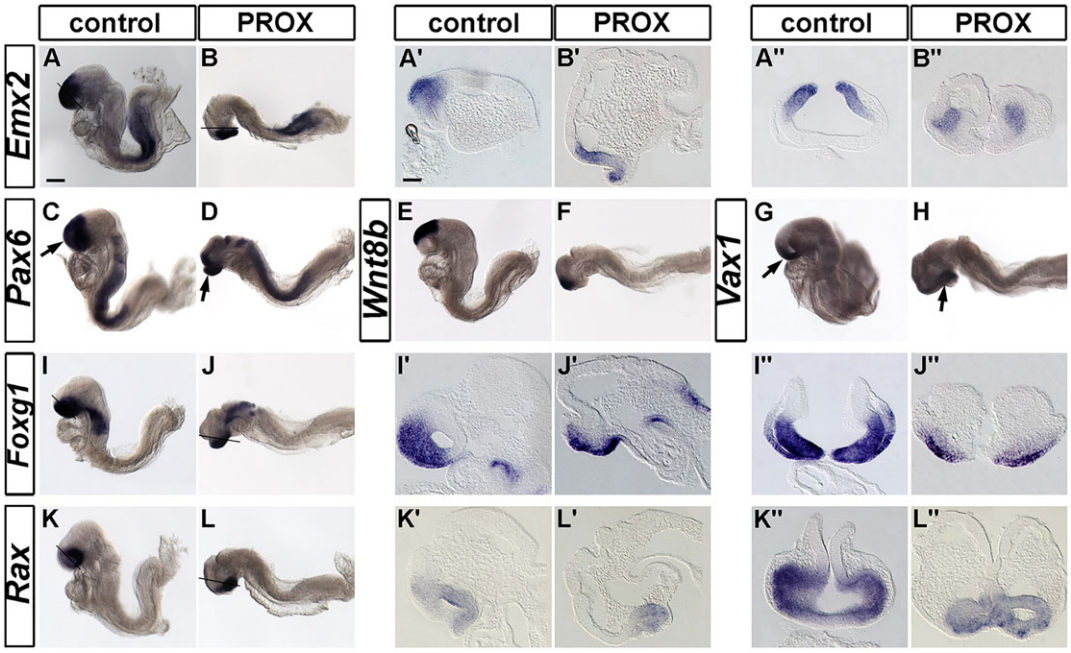

Fig. 5. Comparative analysis of forebrain marker expression in control and ablated mouse embryos. (A-L) Whole-mount images, (A′-L′) longitudinal and (A″-L″) frontal sections of control and PROX embryos cultured for 30 h showing *Emx2*, *Pax6* (arrows in C,D), *Wnt8b*, *Vax1* (arrows in G,H), *Foxg1* and *Rax* expression. Section planes for A″,B″,I″,J″,K″,L″ are indicated in A,B,I,J,K,L. Scale bars: in A, 110 µm for A-L; in A′, 45 µm for A′-L″.

analysed on histological sections by P-HH3 immunodetection. No significant proliferation difference was detected in the neuroectoderm between PROX and control embryos after 12 and 30 h of culture (supplementary material Fig. S4 and Table S1). The severe reduction of the head observed in PROX embryos is not the result of a decrease in cell proliferation.

Alternatively, an increase in cell death could account for the forebrain phenotype. Apoptosis was assessed by TUNEL staining. The overall level of apoptosis was high in both PROX (n=9) and control (n=6) embryos 6 h after manipulation (Fig. 8A,B). After 12 h of culture, apoptosis increased in the ANP of most PROX embryos (n=10/13) contrasting with the decline observed in control embryos (n=8; Fig. 8C,D). After 30 h of culture, apoptosis remained high throughout the cephalic region of the PROX (n=12), as a sixfold increase was observed compared with controls embryos (n=11; Fig. 8E-G; supplementary material Table S1). Remarkably, no difference was detected in the spatial distribution of apoptotic cells within the neuroectoderm of the PROX embryos. The ANR is the region that displayed a higher level of apoptosis in both PROX and control embryos (Fig. 8E′,F′,G).

Interestingly, comparable observations were made in LysoTracker (LT)-stained chick embryos following the removal of the anterior midline ectoderm cells. After just 3 h of culture, a general increase of LT signal was seen in NNE embryos (n=9) and in embryos with a slit in the ectoderm compared with control embryos (n=15) (Fig. 8H-J). After 45 h of culture, high LT staining was still observed in the cephalic region of the NNE embryos (n=12; Fig. 8L) but not in other conditions (n=20 and 14; Fig. 8K,M). These results demonstrate that in both models ablations trigger extensive apoptosis throughout the ANR, the neuroectoderm and prospective CNCCs.

To test whether the head phenotype was due to this increase in cell death, apoptosis was blocked in ablated mouse embryos using the most common pan-caspase inhibitor Z-VAD (Maynard et al., 2000; Weil et al., 1997). TUNEL analysis after 12 and 30 h of culture in presence of Z-VAD showed that, although apoptosis was prevented, the telencephalon territory was not restored (Fig. 9A-D). In addition, no difference in LT staining was found between Z-VAD and DMSO-treated PROX embryos (Fig. 9E,F) showing that cells were not eliminated via another cell death mechanism (Vandenabeele et al., 2006). Finally, the percentage of P-HH3-positive cells in the neuroectoderm after Z-VAD treatment was significantly higher in control compared with PROX embryos at 12 and 30 h of culture (Fig. 9G; supplementary material Table S1; data not shown). This suggests that cells in ablated embryos do not resume a normal pattern of proliferation when saved from apoptosis and that neuroectoderm cell properties are different in PROX and control embryos. In conclusion, the widespread activation of apoptosis in the ANP following the ablation likely accounts for the global head reduction but is not sufficient to explain the specific loss of telencephalon.

Ablation of the proximal anterior midline results in defective BMP, WNT and FGF signalling pathways

BMP, WNT and FGF signalling pathways are known to regulate forebrain development and regionalization. We thus assessed whether the implication of the anterior non-neural ectoderm in ANP development involves these signalling pathways. First, we performed the ablation in the *BRE-lacZ/+* mouse line and analysed the reporter gene as a read-out of the transcriptional activity of the SMAD1/5/8 BMP-effector proteins at the time the head phenotype appears (Monteiro et al., 2004). We found that BMP/SMAD activity was dramatically reduced in the median region of the forming headfold in the PROX embryos after 12 h of culture (n=8; Fig. 10A-D). We also observed that, *Axin2* and *Dkk1*, which are targets of the WNT pathway that function as negative-feedback regulators of WNT signalling, were misexpressed in the head 12 h after ablation (n=7 and n=3, respectively; Fig. 10E-H). We therefore hypothesize that the removal of the non-neural ectoderm leads to an early overactivation of the WNT pathway and a downregulation of BMP/SMAD

Development (2014) 141, 4127-4138 doi:10.1242/dev.107425

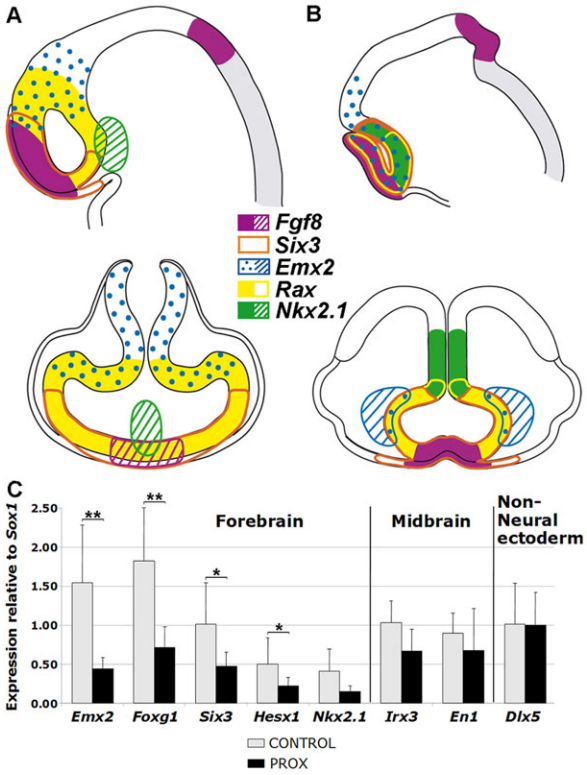

Fig. 6. Summary of the expression pattern analysis and quantitative RT-PCR assays comparing expression in control and ablated mouse embryos. (A,B) Schematic representation of the typical expression domains of *Fgf8*, *Six3* (sections not shown), *Emx2*, *Rax* and *Nkx2.1* genes on longitudinal (top) and frontal (bottom) sections of control (A) and PROX (B) embryos. Hatched colour indicates that the depicted expression domain is outside the plane of section. The hindbrain domain is painted in grey. (C) Quantitative RT-PCR assays measuring RNA levels of the cephalic region of eight individual PROX and eight control embryos cultured for 30 h. For each gene and for a given embryo, values were normalized to the level of expression of *Gapdh* and are presented relative to the level of expression of *Sox1* to show changes in specific subdomains of the neuroectoderm independently of the global loss of neural tissue. The mean values are represented. Error bars indicate s.d. between experimental samples. Wilcoxon test was applied to compare PROX with control embryos. *P*-values were as follow: *Emx2* (**0.007); *Foxg1* (**0.007); *Six3* (*0.015); *Hesx1* (*0.015); *Nkx2.1* (0.058); *Irx3* (0.106); *En1* (0.156); *Dlx5* (0.878).

signalling. Remarkably, this disturbance was transient as the difference in the BMP and WNT signalling did not persist after 30 h of culture, when the head phenotype is well established (n=16 and n=7, respectively; data not shown). As *Fgf8* expression was expanded in the prospective anterior neuroectoderm and ANR of most PROX embryos at 30 h of culture, we examined its onset of expression at the 3- to 4-somite stage. Interestingly, *Fgf8* expression was found enhanced in the headfolds of the PROX embryos after 15 h of culture whereas it was only weakly detected in control embryos (n=6 and n=6, respectively; Fig. 10I-L). We next used pharmacological inhibitors of these signalling pathways in order to mimic or to rescue the PROX phenotype. Unmanipulated embryos cultured in the presence of BMP signalling inhibitor did not show a forebrain truncation (n=34; data not shown). In addition, the presence of pharmacological inhibitors of either the FGF or the WNT pathways did not rescue the forebrain phenotype of PROX embryos after 30 h of culture (n=19 and n=30, respectively; data not shown). This analysis indicates that the removal of the non-neural ectoderm triggers unbalanced activities of BMP, WNT and FGF signalling pathways. However, further experiments will be required to understand (1) how these disturbances lead to the PROX embryo head phenotype and (2) how the BMP, WNT and FGF signalling pathways normally cooperate to regulate forebrain development at the time of neural plate formation.

DISCUSSION

Intact rostral non-neural ectoderm is required for normal forebrain development

In order to elucidate the role of the non-neural ectoderm that abuts the rostralmost neural ectoderm at the early phase of ANP formation, we removed the proximal anterior midline of the late gastrula mouse embryo. Important morphogenetic changes occur in ablated embryos. The cephalic region exhibits an open neuroepithelium with no headfold fusion and develops outside the VYS. Our study focused on the forebrain, which is most severely affected. We showed that the PROX head phenotype does not result from the disruption of known signalling centres such as the AME or the ANR (Camus et al., 2000; Shimamura and Rubenstein, 1997; Withington et al., 2001). The AVE has been shown to be a source of antagonistic signals essential for the development of the head (Perea-Gomez et al., 2001; Stern and Downs, 2012; Thomas and Beddington, 1996). However, at the time of PROX ablation, the AVE is no longer involved in ANP development. Indeed, some AVE cells persist throughout gastrulation but they downregulate AVE markers as their role in protecting ANP from posteriorizing signals is taken over by the AME (Arkell and Tam, 2012; Kwon et al., 2008). Most VE cells contribute to the endoderm layer of the VYS and have an endocytic function essential for nutrient supply before the formation of a functional placenta (Bielinska et al., 1999). Previous literature did not report evidence that development outside the VYS can directly affect anterior neural patterning (Madabhushi and Lacy, 2011; Molkentin et al., 1997). Nevertheless, we cannot rule out the possibility that VYS deficiencies contribute, at least in part, to the head phenotype of PROX embryos (Mao et al., 2010; Zohn and Sarkar, 2010). In chick experiments, the anterior non-neural ectoderm is specifically removed without altering the subjacent endoderm layer at HH4, a developmental stage equivalent to mouse E7.5. As a consequence, the ablated chick embryos developed within the VYS and cardia bifida was never observed. Remarkably, a telencephalon defect similar to that of mouse PROX embryos is observed in these chick embryos. Altogether, these findings indicate that early forebrain development in the mouse and chick embryos depends on the presence of the rostral non-neural ectoderm cells.

Intact rostral non-neural ectoderm is not essential for the specification and maintenance of ectoderm lineages

A reduced allocation of ectoderm cells to the neural plate anteriorly may account for the truncation of the head of PROX embryos. Interestingly, the differentiation potential of isolated ectoderm tissue in response to BMP signalling was recently tested *in vitro* in the mouse (Li et al., 2013). This study showed that the anterior part of the ectoderm layer at OB and EB stages has the potential to become either epidermis or neuroectoderm, depending on the presence or absence of BMP4, respectively. This state is transient because at the EHF stage the ectoderm is no longer responsive to BMP4 and is restricted to either neural or epidermal fate, depending on its original position in the embryo. During gastrulation, several BMP ligands are expressed in the extra-embryonic and anterior regions of the embryo. They are known to act at a distance in adjacent tissues to influence cell fate (Anderson et al., 2002; Bachiller et al., 2000; Solloway and Robertson, 1999; Yang and Klingensmith, 2006). Using *BRE-lacZ/+* mouse embryos, we have previously shown that rostral non-neural ectoderm cells display high

Development (2014) 141, 4127-4138 doi:10.1242/dev.107425

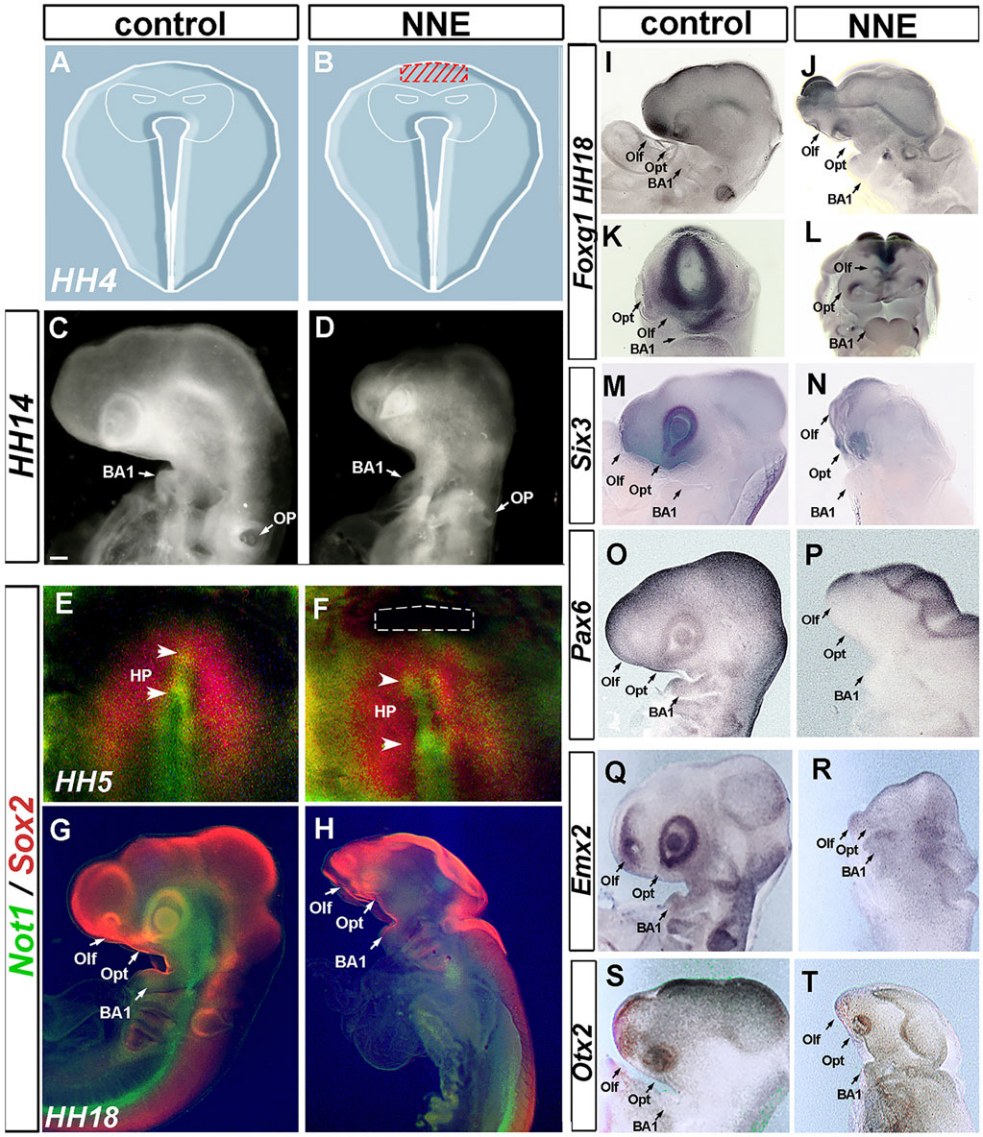

Fig. 7. Ablation of the anterior non-neural ectoderm cells of HH4 chick embryos. Schematic representation at HH4 of untouched control (A) and NNE (B) embryos. The red-hatched zone in B illustrates the area of extirpated anterior non-neural ectoderm. Thin white lines delineate the limits of neural ectoderm, as defined in published fate maps. (C,D) Morphology of the head up to the otic pit of control (C) and NNE (D) embryos developed *in ovo* for 32 h. (E-H) HH5 (E,F) and HH18 (G,H) control (E,G) and NNE (F,H) embryos showing double staining for Not1 (green) and Sox2 (red). NNE ablation (dotted lines) affects neither the formation of head process (Not1; arrowheads) nor the specification of neural ectoderm (Sox2). (I-L) HH18 control lateral (I) and frontal (K), and NNE embryos lateral (J) and frontal (L) views showing *Foxg1* expression. (M,N) HH18 control (M) and NNE (N) chick embryos showing *Six3* expression in the optic vesicles. The telencephalic expression of *Six3* is lost in ablated embryos. (O,P) *Pax6* expression in control (O) and NNE (P) embryos: *Pax6* is confined to neural border after ablation. (Q,R) *Emx2* activity in dorsal telencephalon in control is abolished in NNE embryos. (S,T) *Otx2* expression in forebrain and midbrain becomes restricted to the border of everted brain in NNE, but persists in the optic vesicles. BA1, first branchial arch; HP, head process; Olf, olfactory vesicle; Opt, optic vesicle; OP, otic pit. Scale bar: 150 µm.

BMP signalling at the early phases of neural plate formation (Dobreva et al., 2012), consistent with the expression of BMP direct targets *Id1* and *Id2* in this tissue (Li et al., 2013). Here, we report a downregulation of the BMP signalling pathway in our experimental system that may result into a change of fate of neighbouring cells thus responding to other environmental cues subsequently more preponderant. Our analysis of gene expression pattern revealed no preferential change in the commitment to non-neural or neural fates in the PROX-ablated embryos when they reached EHF stage. In addition, the A-P patterning of the early neural rudiment is established. Therefore, the results are rather suggestive of a deficiency in the subsequent subregionalization of the forebrain territory that may not be induced or maintained.

Rostral non-neural ectoderm cells potentially influence forebrain patterning, but not its survival, by modulating signalling pathways

Extensive apoptosis is observed throughout the ANP of ablated mouse embryos. A moderate to high rate of cell death by apoptosis could reflect the elimination of 'unfit' cells after improper induction or mispatterning (Claveria et al., 2013; Sancho et al., 2013). Remarkably, the level of apoptosis was not higher in prospective forebrain neuroectoderm compared with prospective midbrain. Moreover, no rescue of the telencephalon was observed when apoptosis was prevented in PROX embryos. Taken together, these results indicate that the increase in cell death is not the primary cellular defect responsible for the absence of the telencephalon. In conclusion, our findings support the idea that rostral non-neural ectoderm cells are crucial for further specification of the prospective telencephalon territory rather than for its survival.

Several studies in mouse demonstrated a requirement in the ANP for WNT transcriptional repressors to regulate cell competence, maintain forebrain identity and allow further regionalization (Andoniadou et al., 2007, 2011; Fossat et al., 2011; Lagutin et al., 2003; Lavado et al., 2008). In contrast to what was expected from these studies, no sign of rostral expansion of posterior markers that would suggest a switch in cell identity was observed 30 h after the ablation. Nevertheless, we cannot rule out the possibility that anterior truncation results from an initial posterior transformation of the neuroectoderm subsequently wiped out by apoptosis. Interestingly, we have shown that the removal of the proximal anterior midline triggers an ectopic activation of the WNT signalling pathway in the developing ANP. In zebrafish, the ANB signalling centre secretes SFRPs required during gastrulation to repress WNT signalling in the

Development (2014) 141, 4127-4138 doi:10.1242/dev.107425

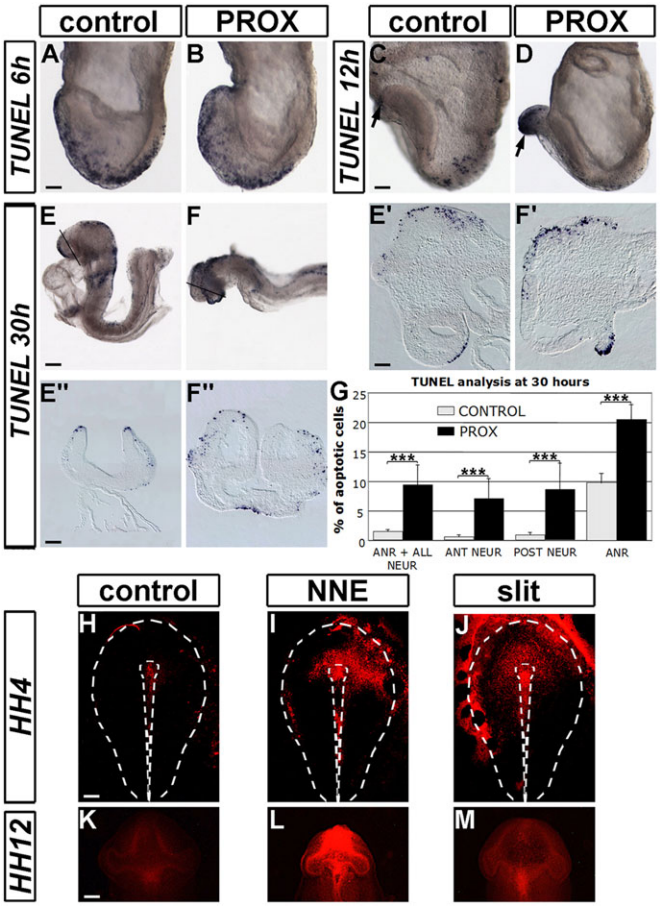

Fig. 8. Distribution and quantification of cell death in ablated mouse and chick embryos. (A-F″) TUNEL assay in whole-mount images (A-F), longitudinal (E′,F′) and frontal (E″,F″) sections showing apoptotic cells in control and PROX embryos cultured for 6, 12 and 30 h. Apoptotic cells are randomly distributed in A and B. Note the remarkably high density of apoptotic cells in the ANP of PROX compared with control embryos (arrows in C,D). (G) Quantification of cell death in the ANR, anterior (ANT NEUR) and posterior (POST NEUR) neuroectoderm in control and PROX embryos cultured for 30 h. ***P<0.001. Data are mean±s.e.m. (H-M) LT staining in unmanipulated control (H,K), NNE (I,L) and 'slit' control (J,M) chick embryos immediately after the manipulation or after 1 day of *in ovo* development. White dotted lines delineate the embryonic region and the primitive streak at the midline (H-J). In K-M, a ventral view of the cephalic region is shown. Scale bars: in A, 70 µm for A,B; in C, 80 µm for C,D; in E, 85 µm for E,F; in E′, 50 µm for E′,F′; in E″, 65 µm for E″,F″; in H, 230 µm for H-J; in K, 150 µm for K-M.

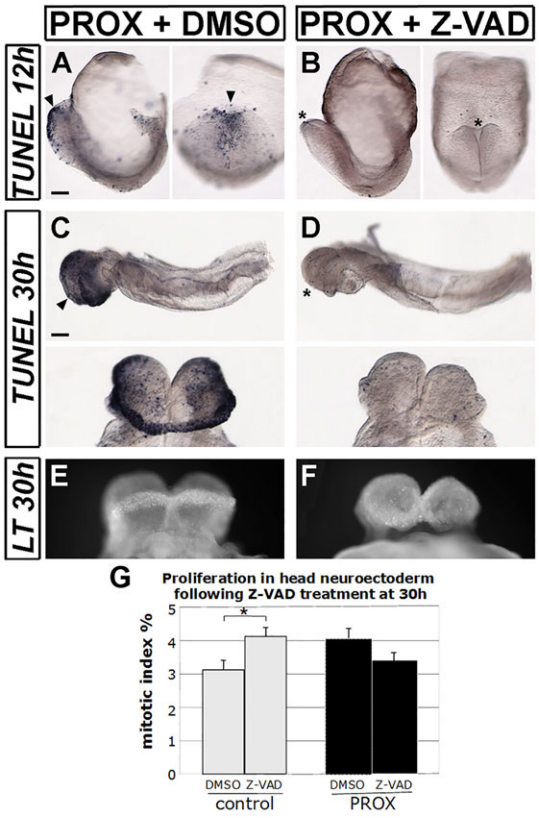

Fig. 9. Effect of the inhibition of apoptosis in ablated mouse embryos. (A-D) TUNEL assay on PROX embryos showing efficient inhibition of apoptosis after 12 (A,B) or 30 h (C,D) of Z-VAD treatment at 150 µM. In A and B, lateral (left) and frontal (right) views are shown. Arrowheads indicate apoptotic cells in the cephalic region and asterisks show their disappearance after Z-VAD treatment. In C,D, lateral view (above) and magnified frontal view (below) of the head, showing severe truncation in DMSO and Z-VAD-treated PROX embryos. (E,F) Ventral view of the cephalic region of LT-stained PROX embryos cultured for 30 h in presence of DMSO or 150 µM of Z-VAD. (G) Quantification of cell proliferation in DMSO- and Z-VAD-treated PROX, and control embryos cultured for 30 h. *P<0.05. Data are mean±s.e.m. Scale bars: in A, 110 µm for A,B; in C, 90 µm for C,D.

developing ANP for the establishment of the telencephalon (Houart et al., 2002). In the mouse, rostral non-neural cells may play a signalling role, like the zebrafish ANB that acts well before the establishment of the secondary organizer ANR.

Finally, we report an enhanced FGF8 signal in the ANP of the PROX embryos that may contribute to their head phenotype. Cross-regulations of the WNT, FGF, BMP and SHH pathways in the forebrain control the morphogenesis of the telencephalon and the eye field (Cho et al., 2013; Danesin et al., 2009; Geach et al., 2014; Gestri et al., 2005; Lupo et al., 2013; Nonomura et al., 2013; Ohkubo et al., 2002; Storm et al., 2006). In particular, BMP signalling mediates A-P patterning within the forebrain itself, with telencephalon specification requiring higher BMP activity than eye development (Barth et al., 1999; Bayramov et al., 2011; Bielen and Houart, 2012). The rostral non-neural ectoderm may regulate several signalling pathways that are important for further regionalization of the forebrain and in particular for the emergence of the telencephalon territory, and may act either directly as a source of signals/antagonists or by transmitting extra-embryonic cues.

In conclusion, this study provides evidence that the rostral non-neural ectoderm is essential for telencephalon development. It opens new perspectives on the role of the neural/non-neural interface and reveals its functional relevance across higher vertebrates.

MATERIALS AND METHODS

Mouse embryo collection and micromanipulation

Embryos from SW×SW, *Gsc+/lacZ×Gsc+/lacZ* (Camus et al., 2000) or SW×*BRE-lacZ/BRE-lacZ* (Monteiro et al., 2004) matings were collected at E7.5. Selected no allantoic bud (OB) or early allantoic bud (EB) stages embryos (Downs and Davies, 1993) displayed a closed amniotic cavity and early signs of neural plate formation. The proximal anterior midline was microsurgically ablated using tungsten needles. The targeted area was approximately 70 µm high (from the extra-embryonic/embryonic junction to a distal position along the midline corresponding to 1/4 of the distance to the node) and 100 µm wide, spanning the midline (about 1/5 of the circumference of the embryo). Experiments were performed in accordance with European and French Agricultural Ministry guidelines for the care and use of laboratory animals (Council directives 2889 and 86/609/EEC).

Development (2014) 141, 4127-4138 doi:10.1242/dev.107425

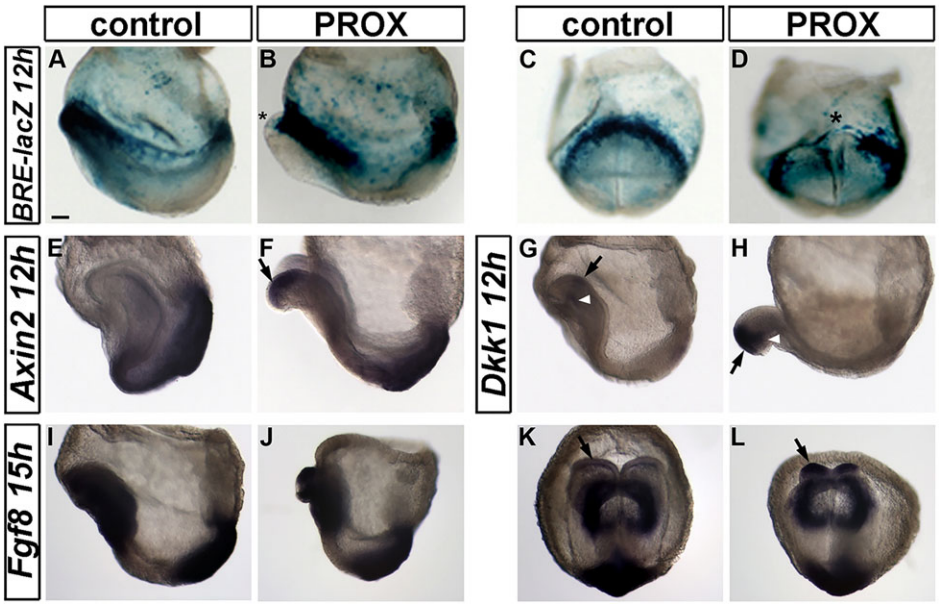

Fig. 10. Effect of removing the proximal anterior midline on BMP, WNT and FGF signalling pathways. (A-L) Whole-mount images in lateral (A,B,E-J) and frontal (C,D,K,L) views of control and PROX embryos cultured for 12 and 15 h. (A-D) Control and PROX *BRE-lacZ*/+ embryos showing β-galactosidase as a read-out of the transcriptional activity of the BMP/SMAD pathway. Asterisks show the reduction of the activity at headfold level in PROX embryos. Ectopic expression of *Axin2* (E,F) and *Dkk1* (G,H) is detected in PROX embryos compared with control (black arrows). *Dkk1* expression is normal in the ADE (white arrowheads). *Fgf8* expression in the headfolds (arrows) is enhanced in PROX embryos. Scale bar: 80 µm in A-L.

Mouse embryo culture

Ablated and control embryos were cultured *in vitro* in 75% rat serum in 25% DMEM at 37°C and 5% CO_2 (Rivera-Perez et al., 2010). Embryos reached the early headfold (EHF), the pre-somitic to three-somite stage, and the 7- to 12-somite stage after, respectively, 6, 12 and 24-30 h of culture. In control embryos, development proceeded normally, as judged by heart and head morphogenesis.

DMSO-diluted chemical inhibitors were used at these concentrations in static culture: Z-VAD-FMK (Bachem), 100 to 150 µM; MEK inhibitor PD0325901 (Axon Medchem), 1 to 15 µM; WNT inhibitor endo-IWR1 (Tocris Bioscience), 50 to 100 µM; and canonical and non-Smad-mediated BMP signalling inhibitor dorsomorphin (Sigma), 1 to 10 µM. Equivalent volumes of DMSO were added in control experiments.

Chick embryo collection and culture

Fertilized chick eggs were incubated at 38°C for 18 h and staged according to Hamburger and Hamilton (1992). HH4 embryos were operated using glass microscalpels. The ablated non-neural ectoderm (NNE) territory corresponded to the anteriormost third of the space lying between Hensen's Node and the limit of the *area opaca*, and extended bilaterally to 30°. 'Slit' series consisted in an incision of the caudal limit of NNE. Operations were performed through the vitelline membrane, and strictly restricted to the ectoderm. After the operation, embryos developed *in ovo* until they reached from HH12 to HH18 stages (16-36 somites).

Whole-mount *in situ* hybridization, β-galactosidase staining, and histology

Whole-mount *in situ* hybridization was performed on 4% paraformaldehyde (PFA) fixed specimens (from 4 to 17 for each antisense riboprobes and each experimental condition). Whole-mount *in situ* hybridization and β-galactosidase detection were performed according to a standard method (Camus et al., 2006). Embryos were cryosectioned at 20 µm.

Cell proliferation

Phospho-Histone H3 (P-HH3) was immunodetected on embryos cryosectioned at 20 µm and incubated for 2 h at room temperature in 10% FCS, 0.2% Triton X-100 in PBS, and overnight at 4°C in rabbit anti-P-HH3 (1/500; 06-570, Upstate Biotechnology) in 1% FCS, 0.2% Triton X-100 in PBS. After three washes, sections were incubated for 2 h at room temperature in donkey anti-rabbit peroxydase (1/500; sc-2313, Santa Cruz Biotechnology) before staining with DAB (Sigma).

LysoTracker Red (LT) staining and TUNEL assay

Living mouse embryos were incubated for 30 min at 37°C in DMEM, 5% FCS and 25 mM HEPES, containing 5 µM LT (L7528, Invitrogen). Chick embryos were stained *ex ovo* for 20 min at room temperature in PBS containing 2.5 µM LT. TUNEL assay was performed using the ApopTag Peroxidase In Situ Apoptosis Detection Kit (Millipore). In preliminary experiments, we found that LT and TUNEL analysis revealed similar profiles in embryos developed *in vitro* (Zucker et al., 1998 and data not shown).

Quantification of neuroectoderm, mitotic and apoptotic cells

As no difference in neuroectoderm cell number per μm^2 was found between ablated (n=7) and control (n=6) embryos cultured for 30 h, quantification was carried out by measuring neuroectoderm surface, on longitudinal sections (ImageJ software). P-HH3-positive cells were counted manually in prospective forebrain (up to the posterior limit of the *Emx2* expression domain) and midbrain (from the posterior limit of the *Emx2* expression domain up to the *Fgf8*-positive isthmus) neuroectoderm. TUNEL-positive cells were counted in the non-neural part of the ANR, in forebrain and midbrain neuroectoderm (with the same limits as above). Quantifications were performed on average on five embryos per condition (with 3 to 8 sections per embryo). The percentage of apoptotic and mitotic cells was calculated using an average cell surface determined by measuring the surface of over 100 cells for each developmental stage (25 μm^2 after 12 h of culture and 36 μm^2 after 30 h). *t*-tests were applied to the quantification data.

Quantitative analysis of gene expression

RT-PCR assays were performed using the primer sequences and the method described by Camus et al. (2006). Additional primer sequences were obtained from Primer Bank (Wang and Seed, 2003): *Dlx5* 9294722a1; *Emx2* 28372477a3; *Irx3* 6680472a2; *Six3* 258613883c2. cDNA sample of the cephalic part anterior to the second somite of a 10-somite stage wild-type embryo was the calibrator used as the basis for comparative results.

Acknowledgements

We are indebted to the ImagoSeine platform and to the IJM animal facility staff for excellent technical assistance. We thank G. Duval and S. Pozzi for embryo culture work; C. L. Mummery for BRE-LacZ mice; C. Houart, J. P. Martinez-Barbera and A. Pierani for advice and discussion; and A. Perea-Gomez and F. Causeret for critical reading of the manuscript.

Competing interests

The authors declare no competing financial interests.

Author contributions

A.C. conceived and coordinated the project; A.C., M.C. and S.E.C. designed experiments; A.C., M.C., C.P. and D.S.-D. performed mouse experiments ; S.E.C. performed chick experiments; S.M.C.d.S.L. provided the *BRE-LacZ* tool; M.C., A.C.

and A.Z. analysed the data; A.C. wrote the manuscript with contributions of M.C., S.E.C., C.P., A.Z., D.S.-D. and J.C.

Funding

This work was supported by the Centre National de la Recherche Scientifique and The Agence National pour la Recherche [ANR-09-BLAN-0153 to S.C. and AFSR 2012.05 to S.C.]. Vlaams Instituut voor Biotechnologie supported A.Z. The Netherlands organization of Scientific Research (NWO) [ASPASIA 015.007.037] and the Interuniversity Attraction Poles (PAI) [P7/07] supported S.M.C.d.S.L. M.C. was funded by a fellowship from the Ministère de l'Enseignement Supérieur et de la Recherche and C.P. by a fellowship from the Fondation pour la Recherche Médicale and the Agence National pour la Recherche.

Supplementary material

Supplementary material available online at
http://dev.biologists.org/lookup/suppl/doi:10.1242/dev.107425/-/DC1

References

Anderson, R. M., Lawrence, A. R., Stottmann, R. W., Bachiller, D. and Klingensmith, J. (2002). Chordin and noggin promote organizing centers of forebrain development in the mouse. *Development* **129**, 4975-4987.

Andoniadou, C. L. and Martinez-Barbera, J. P. (2013). Developmental mechanisms directing early anterior forebrain specification in vertebrates. *Cell. Mol. Life Sci.* **70**, 3739-3752.

Andoniadou, C. L., Signore, M., Sajedi, E., Gaston-Massuet, C., Kelberman, D., Burns, A. J., Itasaki, N., Dattani, M. and Martinez-Barbera, J. P. (2007). Lack of the murine homeobox gene Hesx1 leads to a posterior transformation of the anterior forebrain. *Development* **134**, 1499-1508.

Andoniadou, C. L., Signore, M., Young, R. M., Gaston-Massuet, C., Wilson, S. W., Fuchs, E. and Martinez-Barbera, J. P. (2011). HESX1- and TCF3-mediated repression of Wnt/beta-catenin targets is required for normal development of the anterior forebrain. *Development* **138**, 4931-4942.

Arkell, R. M. and Tam, P. P. L. (2012). Initiating head development in mouse embryos: integrating signalling and transcriptional activity. *Open Biol.* **2**, 120030.

Arkell, R. M., Fossat, N. and Tam, P. P. L. (2013). Wnt signalling in mouse gastrulation and anterior development: new players in the pathway and signal output. *Curr. Opin. Genet. Dev.* **23**, 454-460.

Bachiller, D., Klingensmith, J., Kemp, C., Belo, J. A., Anderson, R. M., May, S. R., McMahon, J. A., McMahon, A. P., Harland, R. M., Rossant, J. et al. (2000). The organizer factors Chordin and Noggin are required for mouse forebrain development. *Nature* **403**, 658-661.

Barth, K. A., Kishimoto, Y., Rohr, K. B., Seydler, C., Schulte-Merker, S. and Wilson, S. W. (1999). Bmp activity establishes a gradient of positional information throughout the entire neural plate. *Development* **126**, 4977-4987.

Bayramov, A. V., Eroshkin, F. M., Martynova, N. Y., Ermakova, G. V., Solovieva, E. A. and Zaraisky, A. G. (2011). Novel functions of Noggin proteins: inhibition of Activin/Nodal and Wnt signaling. *Development* **138**, 5345-5356.

Bielen, H. and Houart, C. (2012). BMP signaling protects telencephalic fate by repressing eye identity and its Cxcr4-dependent morphogenesis. *Dev. Cell* **23**, 812-822.

Bielinska, M., Narita, N. and Wilson, D. B. (1999). Distinct roles for visceral endoderm during embryonic mouse development. *Int. J. Dev. Biol.* **43**, 183-205.

Braun, M. M., Etheridge, A., Bernard, A., Robertson, C. P. and Roelink, H. (2003). Wnt signaling is required at distinct stages of development for the induction of the posterior forebrain. *Development* **130**, 5579-5587.

Cajal, M., Lawson, K. A., Hill, B., Moreau, A., Rao, J., Ross, A., Collignon, J. and Camus, A. (2012). Clonal and molecular analysis of the prospective anterior neural boundary in the mouse embryo. *Development* **139**, 423-436.

Camus, A., Davidson, B. P., Billiards, S., Khoo, P., Rivera-Perez, J. A., Wakamiya, M., Behringer, R. R. and Tam, P. P. (2000). The morphogenetic role of midline mesendoderm and ectoderm in the development of the forebrain and the midbrain of the mouse embryo. *Development* **127**, 1799-1813.

Camus, A., Perea-Gomez, A., Moreau, A. and Collignon, J. (2006). Absence of Nodal signaling promotes precocious neural differentiation in the mouse embryo. *Dev. Biol.* **295**, 743-755.

Carmona-Fontaine, C., Acuña, G., Ellwanger, K., Niehrs, C. and Mayor, R. (2007). Neural crests are actively precluded from the anterior neural fold by a novel inhibitory mechanism dependent on Dickkopf1 secreted by the prechordal mesoderm. *Dev. Biol.* **309**, 208-221.

Cho, G.-S., Choi, S.-C. and Han, J.-K. (2013). BMP signal attenuates FGF pathway in anteroposterior neural patterning. *Biochem. Biophys. Res. Commun.* **434**, 509-515.

Clavería, C., Giovinazzo, G., Sierra, R.Torres, M. (2013). Myc-driven endogenous cell competition in the early mammalian embryo. *Nature* **500**, 39-44.

Collignon, J., Varlet, I., Robertson, E. J. (1996). Relationship between asymmetric nodal expression and the direction of embryonic turning. *Nature* **381**, 155-158.

Creuzet, S. E. (2009). Neural crest contribution to forebrain development. *Semin. Cell Dev. Biol.* **20**, 751-759.

Danesin, C., Peres, J. N., Johansson, M., Snowden, V., Cording, A., Papalopulu, N. and Houart, C. (2009). Integration of telencephalic Wnt and hedgehog signaling center activities by Foxg1. *Dev. Cell* **16**, 576-587.

del Barco Barrantes, I., Davidson, G., Gröne, H.-J., Westphal, H. and Niehrs, C. (2003). Dkk1 and noggin cooperate in mammalian head induction. *Genes Dev.* **17**, 2239-2244.

Dobreva, M. P., Lhoest, L., Pereira, P. N. G., Umans, L., Camus, A., Chuva de Sousa Lopes, S. M. and Zwijsen, A. (2012). Periostin as a biomarker of the amniotic membrane. *Stem Cells Int.* **2012**, 987185.

Downs, K. M. and Davies, T. (1993). Staging of gastrulating mouse embryos by morphological landmarks in the dissecting microscope. *Development* **118**, 1255-1266.

Eagleson, G. W. and Dempewolf, R. D. (2002). The role of the anterior neural ridge and Fgf-8 in early forebrain patterning and regionalization in Xenopus laevis. *Comp. Biochem. Physiol. B Biochem. Mol. Biol.* **132**, 179-189.

Ezin, A. M., Fraser, S. E. and Bronner-Fraser, M. (2009). Fate map and morphogenesis of presumptive neural crest and dorsal neural tube. *Dev. Biol.* **330**, 221-236.

Fernandez-Garre, P., Rodriguez-Gallardo, L., Gallego-Diaz, V., Alvarez, I. S. and Puelles, L. (2002). Fate map of the chicken neural plate at stage 4. *Development* **129**, 2807-2822.

Fossat, N., Jones, V., Khoo, P.-L., Bogani, D., Hardy, A., Steiner, K., Mukhopadhyay, M., Westphal, H., Nolan, P. M., Arkell, R. et al. (2011). Stringent requirement of a proper level of canonical WNT signalling activity for head formation in mouse embryo. *Development* **138**, 667-676.

Geach, T. J., Faas, L., Devader, C., Gonzalez-Cordero, A., Tabler, J. M., Brunsdon, H., Isaacs, H. V. and Dale, L. (2014). An essential role for LPA signalling in telencephalon development. *Development* **141**, 940-949.

Gestri, G., Carl, M., Appolloni, I., Wilson, S. W., Barsacchi, G. and Andreazzoli, M. (2005). Six3 functions in anterior neural plate specification by promoting cell proliferation and inhibiting Bmp4 expression. *Development* **132**, 2401-2413.

Hallonet, M., Kaestner, K. H., Martin-Parras, L., Sasaki, H., Betz, U. A. K. and Ang, S.-L. (2002). Maintenance of the specification of the anterior definitive endoderm and forebrain depends on the axial mesendoderm: a study using HNF3beta/Foxa2 conditional mutants. *Dev. Biol.* **243**, 20-33.

Hamburger, V. and Hamilton, H. L. (1992). A series of normal stages in the development of the chick embryo. *Dev. Dyn.* **195**, 231-272.

Houart, C., Westerfield, M. and Wilson, S. W. (1998). A small population of anterior cells patterns the forebrain during zebrafish gastrulation. *Nature* **391**, 788-792.

Houart, C., Caneparo, L., Heisenberg, C.-P., Barth, K. A., Take-Uchi, M. and Wilson, S.W. (2002). Establishment of the telencephalon during gastrulation by local antagonism of Wnt signaling. *Neuron* **35**, 255-265.

Kiecker, C. and Lumsden, A. (2012). The role of organizers in patterning the nervous system. *Annu. Rev. Neurosci.* **35**, 347-367.

Khudyakov, J. and Bronner-Fraser, M. (2009). Comprehensive spatiotemporal analysis of early chick neural crest network genes. *Dev. Dyn.* **238**, 716-723.

Kobayashi, D., Kobayashi, M., Matsumoto, K., Ogura, T., Nakafuku, M. and Shimamura, K. (2002). Early subdivisions in the neural plate define distinct competence for inductive signals. *Development* **129**, 83-93.

Kwon, G. S., Viotti, M. and Hadjantonakis, A.-K. (2008). The endoderm of the mouse embryo arises by dynamic widespread intercalation of embryonic and extraembryonic lineages. *Dev. Cell* **15**, 509-520.

Lagutin, O. V., Zhu, C. C., Kobayashi, D., Topczewski, J., Shimamura, K., Puelles, L., Russell, H. R. C., McKinnon, P. J., Solnica-Krezel, L. and Oliver, G. (2003). Six3 repression of Wnt signaling in the anterior neuroectoderm is essential for vertebrate forebrain development. *Genes Dev.* **17**, 368-379.

Lavado, A., Lagutin, O. V. and Oliver, G. (2008). Six3 inactivation causes progressive caudalization and aberrant patterning of the mammalian diencephalon. *Development* **135**, 441-450.

Li, L., Liu, C., Biechele, S., Zhu, Q., Song, L., Lanner, F., Jing, N. and Rossant, J. (2013). Location of transient ectodermal progenitor potential in mouse development. *Development* **140**, 4533-4543.

Lupo, G., Novorol, C., Smith, J. R., Vallier, L., Miranda, E., Alexander, M., Biagioni, S., Pedersen, R. A. and Harris, W. A. (2013). Multiple roles of Activin/Nodal, bone morphogenetic protein, fibroblast growth factor and Wnt/beta-catenin signalling in the anterior neural patterning of adherent human embryonic stem cell cultures. *Open Biol.* **3**, 120167.

Madabhushi, M. and Lacy, E. (2011). Anterior visceral endoderm directs ventral morphogenesis and placement of head and heart via BMP2 expression. *Dev. Cell* **21**, 907-919.

Mao, J., McKean, D. M., Warrier, S., Corbin, J. G., Niswander, L. and Zohn, I. E. (2010). The iron exporter ferroportin 1 is essential for development of the mouse embryo, forebrain patterning and neural tube closure. *Development* **137**, 3079-3088.

Maretto, S., Müller, P.-S., Aricescu, A. R., Cho, K. W. Y., Bikoff, E. K. and Robertson, E. J. (2008). Ventral closure, headfold fusion and definitive endoderm migration defects in mouse embryos lacking the fibronectin leucine-rich transmembrane protein FLRT3. *Dev. Biol.* **318**, 184-193.

Martinez Barbera, J. P., Clements, M., Thomas, P., Rodriguez, T., Meloy, D., Kioussis, D. and Beddington, R. S. (2000). The homeobox gene Hex is required in definitive endodermal tissues for normal forebrain, liver and thyroid formation. *Development* **127**, 2433-2445.

Maynard, T. M., Wakamatsu, Y. and Weston, J. A. (2000). Cell interactions within nascent neural crest cell populations transiently promote death of neurogenic precursors. *Development* **127**, 4561-4572.

Molkentin, J. D., Lin, Q., Duncan, S. A. and Olson, E. N. (1997). Requirement of the transcription factor GATA4 for heart tube formation and ventral morphogenesis. *Genes Dev.* **11**, 1061-1072.

Monteiro, R. M., de Sousa Lopes, S. M. C., Korchynskyi, O., ten Dijke, P. and Mummery, C. L. (2004). Spatio-temporal activation of Smad1 and Smad5 in vivo: monitoring transcriptional activity of Smad proteins. *J. Cell Sci.* **117**, 4653-4663.

Nonomura, K., Yamaguchi, Y., Hamachi, M., Koike, M., Uchiyama, Y., Nakazato, K., Mochizuki, A., Sakaue-Sawano, A., Miyawaki, A., Yoshida, H. et al. (2013). Local apoptosis modulates early mammalian brain development through the elimination of morphogen-producing cells. *Dev. Cell* **27**, 621-634.

Ohkubo, Y., Chiang, C. and Rubenstein, J. L. R. (2002). Coordinate regulation and synergistic actions of BMP4, SHH and FGF8 in the rostral prosencephalon regulate morphogenesis of the telencephalic and optic vesicles. *Neuroscience* **111**, 1-17.

Paek, H., Hwang, J. Y., Zukin, R. S. and Hébert, J. M. (2011). β-Catenin-dependent FGF signaling sustains cell survival in the anterior embryonic head by countering Smad4. *Dev. Cell.* **20**, 689-699.

Papalopulu, N. and Kintner, C. (1993). Xenopus Distal-less related homeobox genes are expressed in the developing forebrain and are induced by planar signals. *Development* **117**, 961-975.

Patthey, C. and Gunhaga, L. (2011). Specification and regionalisation of the neural plate border. *Eur. J. Neurosci.* **34**, 1516-1528.

Perea-Gomez, A., Rhinn, M. and Ang, S. L. (2001). Role of the anterior visceral endoderm in restricting posterior signals in the mouse embryo. *Int. J. Dev. Biol.* **45**, 311-320.

Puelles, L., Fernández-Garre, P., Sánchez-Arrones, L., García-Calero, E. and Rodríguez-Gallardo, L. (2005). Correlation of a chicken stage 4 neural plate fate map with early gene expression patterns. *Brain Res. Rev.* **49**, 167-178.

Rivera-Pérez, J. A., Jones, V. and Tam, P. P. L. (2010). Culture of whole mouse embryos at early postimplantation to organogenesis stages: developmental staging and methods. *Methods Enzymol.* **476**, 185-203.

Sánchez-Arrones, L., Ferrán, J. L., Rodriguez-Gallardo, L. and Puelles, L. (2009). Incipient forebrain boundaries traced by differential gene expression and fate mapping in the chick neural plate. *Dev. Biol.* **335**, 43-65.

Sanchez-Arrones, L., Stern, C. D., Bovolenta, P. and Puelles, L. (2012). Sharpening of the anterior neural border in the chick by rostral endoderm signalling. *Development* **139**, 1034-1044.

Sancho, M., Di-Gregorio, A., George, N., Pozzi, S., Sánchez, J. M., Pernaute, B. and Rodríguez, T. A. (2013). Competitive interactions eliminate unfit embryonic stem cells at the onset of differentiation. *Dev. Cell* **26**, 19-30.

Selleck, M. A. and Bronner-Fraser, M. (1995). Origins of the avian neural crest: the role of neural plate-epidermal interactions. *Development* **121**, 525-538.

Shawlot, W., Wakamiya, M., Kwan, K. M., Kania, A., Jessell, T. M. and Behringer, R. R. (1999). Lim1 is required in both primitive streak-derived tissues and visceral endoderm for head formation in the mouse. *Development* **126**, 4925-4932.

Shimamura, K. and Rubenstein, J. L. (1997). Inductive interactions direct early regionalization of the mouse forebrain. *Development* **124**, 2709-2718.

Solloway, M. J. and Robertson, E. J. (1999). Early embryonic lethality in Bmp5; Bmp7 double mutant mice suggests functional redundancy within the 60A subgroup. *Development* **126**, 1753-1768.

Stern, C. D. and Downs, K. M. (2012). The hypoblast (visceral endoderm): an evo-devo perspective. *Development* **139**, 1059-1069.

Storm, E. E., Garel, S., Borello, U., Hebert, J. M., Martinez, S., McConnell, S. K., Martin, G. R. and Rubenstein, J. L. R. (2006). Dose-dependent functions of Fgf8 in regulating telencephalic patterning centers. *Development* **133**, 1831-1844.

Streit, A. (2004). Early development of the cranial sensory nervous system: from a common field to individual placodes. *Dev. Biol.* **276**, 1-15.

Thomas, P. and Beddington, R. (1996). Anterior primitive endoderm may be responsible for patterning the anterior neural plate in the mouse embryo. *Curr. Biol.* **6**, 1487-1496.

Vandenabeele, P., Vanden Berghe, T. and Festjens, N. (2006). Caspase inhibitors promote alternative cell death pathways. *Sci. STKE* **2006**, pe44.

Vieira, C., Pombero, A., Garcia-Lopez, R., Gimeno, L., Echevarria, D. and Martinez, S. (2010). Molecular mechanisms controlling brain development: an overview of neuroepithelial secondary organizers. *Int. J. Dev. Biol.* **54**, 7-20.

Wang, X. and Seed, B. (2003). A PCR primer bank for quantitative gene expression analysis. *Nucleic Acids Res.* **31**, e154.

Weil, M., Jacobson, M. D. and Raff, M. C. (1997). Is programmed cell death required for neural tube closure? *Curr. Biol.* **7**, 281-284.

Wilson, S. W. and Houart, C. (2004). Early steps in the development of the forebrain. *Dev. Cell* **6**, 167-181.

Withington, S., Beddington, R. and Cooke, J. (2001). Foregut endoderm is required at head process stages for anteriormost neural patterning in chick. *Development* **128**, 309-320.

Yang, Y.-P. and Klingensmith, J. (2006). Roles of organizer factors and BMP antagonism in mammalian forebrain establishment. *Dev. Biol.* **296**, 458-475.

Ye, W., Shimamura, K., Rubenstein, J. L. R., Hynes, M. A. and Rosenthal, A. (1998). FGF and Shh signals control dopaminergic and serotonergic cell fate in the anterior neural plate. *Cell* **93**, 755-766.

Zohn, I. E. and Sarkar, A. A. (2010). The visceral yolk sac endoderm provides for absorption of nutrients to the embryo during neurulation. *Birth Defects Res. A Clin. Mol. Teratol.* **88**, 593-600.

Zucker, R. M., Hunter, S. and Rogers, J. M. (1998). Confocal laser scanning microscopy of apoptosis in organogenesis-stage mouse embryos. *Cytometry* **33**, 348-354.

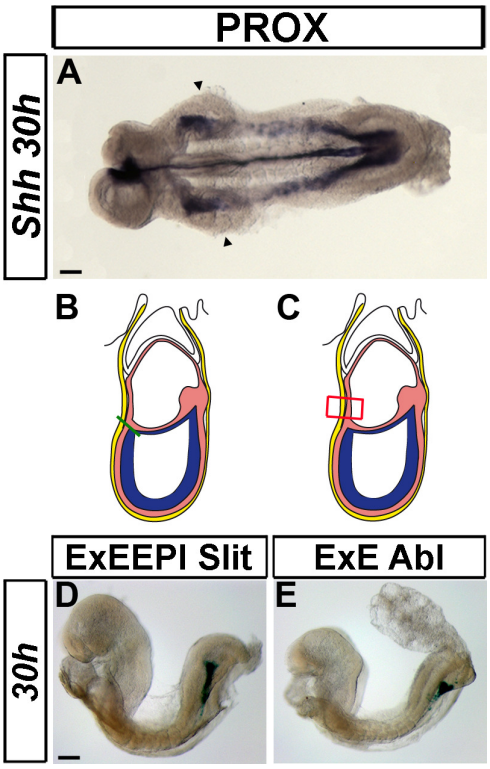

Fig. S1. (A) Ventral view of a PROX embryo cultured for 30 hours (anterior to the left) after *Shh* WISH. Note that foregut invagination is taking place, but the gut endoderm and the body wall fail to fuse at the ventral midline (as described in mutant FLRT 3-/- embryos by Maretto et al., 2008). Consequently, the induced precardiac mesoderm forms two separate lateral heart rudiments (arrowheads) residing appropriately posterior to the headfolds. **(B,C)** Schematic representations of control micromanipulations in OB/EB stage embryos: (B) a lateral cut (green bar) is performed at the extraembryonic/embryonic boundary (ExEEPI Slit) and (C) the anterior distal midline region of extraembryonic tissues the size of the PROX ablation is removed (red square; ExE Abl). **(D,E)** 30h-cultured ExEEPI Slit and ExE Abl embryos developed normally. These experiments were performed in *Nodal*$^{lacZ/+}$ embryos thus β-galactosidase staining is seen in the residual node (Collignon et al., 1996). Scale bars: 60 μm in A and 110 μm in D-E.

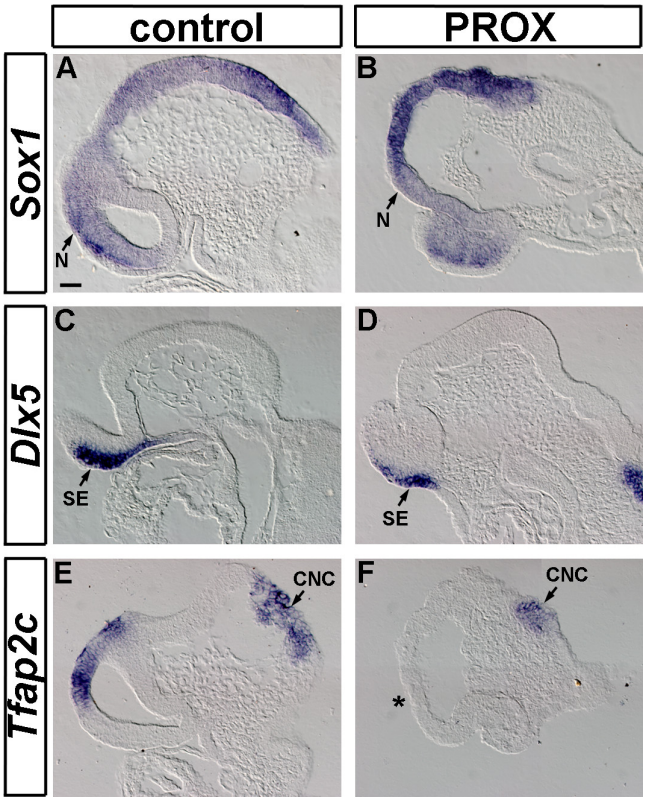

Fig. S2. (**A-F**) Longitudinal histological sections of control (A,C,E) and PROX (B,D,F) embryos cultured for 30 hours showing *Sox1* (A,B), *Dlx5* (C,D) and *Tfap2c* (E,F) expression. Note in the control, *Tfap2c* expression in the dorsal part of the forebrain and its absence in the PROX embryo (asterisk). N: neuroectoderm; SE: surface ectoderm; CNC: cephalic neural crest. Scale bar: 30 µm.

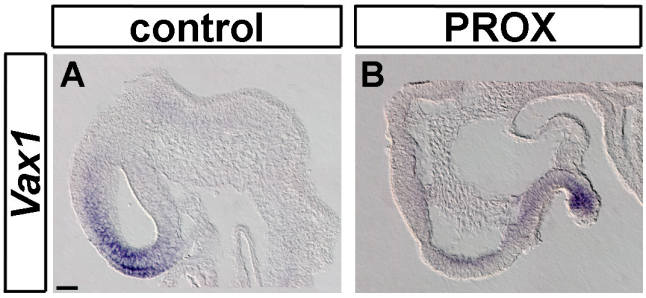

Fig. S3. (**A,B**) Longitudinal histological sections of control and PROX mouse embryos cultured for 30 hours showing *Vax1* expression in forebrain neuroectoderm, ANR and prospective olfactory placode ectoderm. Scale bar: 50 µm.

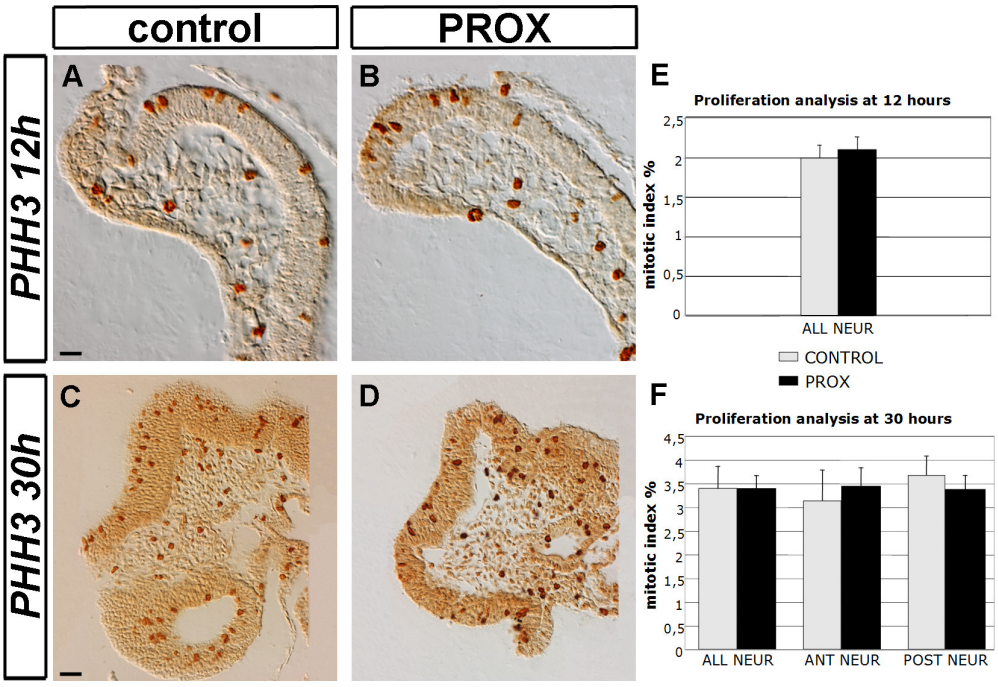

Fig. S4. (A-D) P-HH3 immunodetection on longitudinal histological sections of control (A,C) and PROX (B,D) embryos cultured for 12 and 30 hours. The section of the control in C was rotated 90° anticlockwise to ease the comparison. (**E,F**) Mitotic index in head neuroectoderm (ALL NEUR), anterior (ANT NEUR) and posterior (POST NEUR) neuroectoderm of control and PROX embryos cultured for 12 (E) and 30 hours (F). Note that at 30 hours (F) the small increase in percentage found in the anterior neuroectoderm of PROX embryos is counterbalanced by the reduction observed in the posterior neuroectoderm. Data are mean±s.e.m. Scale bars: 20 µm in A-B; 35 µm in C-D.

Table S1: Percentage of P-HH3- and TUNEL-positive cells in presumed forebrain and midbrain neuroectoderm. All results are mean ±s.e.m.. See Materials and methods for a description of methods used. Note that high s.e.m. values reflect the variation of the severity of the head truncation in PROX embryos.

Table S1: P-HH3 and TUNEL analysis in the ANP

Marker assayed	Embryo manipulation	Number of embryos (number of sections)	ANR	Forebrain neuroectoderm	Midbrain neuroectoderm	Forebrain and midbrain neuroectoderm
P-HH3	PROX 12h	5 (42)				2.10±0.15
P-HH3	CONTROL 12h	5 (45)				1.97±0.17
P-HH3	PROX 30h	6 (36)		3.45±0.37	3.38±0.30	3.40±0.25
P-HH3	CONTROL 30h	4 (14)		3.14±0.63	3.68±0.39	3.40±0.44
TUNEL	PROX 30h	4 (17)	20.50±2.38 [0.001]	7.17±3.28 [0.001]	8.64±4.43 [0.001]	9.54±3.23 [0.001]*
TUNEL	CONTROL 30h	6 (18)	9.80±1.37	0.59±0.19	0.93±0.22	1.52±0.14*
P-HH3	PROX 30h + DMSO	6 (23)				4.02±0.30
P-HH3	PROX 30h + Z-VAD	4 (20)				3.41±0.20
P-HH3	CONTROL 30h + DMSO	4 (17)				3.08±0.29 [0.05]
P-HH3	CONTROL 30h + Z-VAD	3 (12)				4.12±0.24

*Quantification includes the area of the ANR. *P*-values are provided in square parentheses when the difference between manipulated or Z-VAD-treated embryos and controls was significant according to Student's *t*-test.